IET Science, Measurement & Technology

Research Article

IET Journals
The Institution of Engineering and Technology

Space charge and conductivity measurement of XLPE nanocomposites for HVDC insulation–permittivity as a nanofiller selection parameter

ISSN 1751-8822
Received on 12th January 2018
Revised 19th June 2018
Accepted on 31st July 2018
E-First on 17th September 2018
doi: 10.1049/iet-smt.2018.5134
www.ietdl.org

Paramane Ashish Sharad[1], Kannaiah Sathish Kumar[1] ✉, Mohd Hafizi Ahmad[2], Mohamed Afendi Mohamed Piah[2]

[1]*School of Electrical Engineering, Vellore Institute of Technology, Vellore, TN 632014, India*

[2]*Institute of High Voltage & High Current, School of Electrical Engineering, Faculty of Electrical Engineering, Universiti Teknologi Malaysia, Johor 81310, Malaysia*

✉ *E-mail: ksathishkumar@vit.ac.in*

Abstract: Cross-linked polyethylene (XLPE) insulation is successfully used for high-voltage AC transmission. However, it is still under development for high-voltage DC application due to space charge accumulation, which distorts the internal electrical field distribution and leads to its aging/failure. Therefore, the space charge should be measured and carefully analysed. On the other side, conductivity measurement helps to forecast the degradation probability of the insulation. Higher conductivity represents the severe degradation. Nanofiller addition, such as SiO_2, TiO_2, MgO and so on (<5 wt%), particularly surface-modified nanofiller due to its better dispersion significantly suppresses the space charge accumulation and conductivity. Nevertheless, the choice of suitable nanofiller has still remained a challenge. With this context, space charge and conductivity of XLPE-silica and XLPE-magnesium oxide (MgO) surface-modified nanocomposites are measured. This study proposes a parameter for nanofiller selection that will deliver optimal properties for the intended application. Results show that nanocomposites with higher nanofiller permittivity (i.e. MgO) have less space charge accumulation and low conductivity and are justified with the help of a band gap theory model.

1 Introduction

DC voltage application to cross-linked polyethylene (XLPE) insulation leads to the space charge formation due to dielectric polarisation and relaxation phenomenon. Space charge is generally formed due to the imbalanced injection and extraction of the charge carriers (electrons) at the anode and cathode. Hence, it can also refer as surplus charge present inside the insulation. Depends on the type of space charge developed inside the insulation, i.e. homo-charge (same polarity as that of the adjacent electrode) or hetero-charge (opposite polarity as that of the adjacent electrode), the electrical field increases or decreases, respectively, which causes its aging [1–3]. Byproducts of the cross-linking reaction of XLPE affect the polarity of space charge [4].

Also, the DC voltage application leads to the flow of current due to polarisation (i.e. polarisation current) of the insulation. When the DC supply is switched-off and insulation is short-circuited, depolarisation current flows. The difference between polarisation and depolarisation currents is called as conduction (or absorption or leakage) current, which is directly proportional to the conductivity. Higher the conduction current more will be the conductivity and more likely is the degradation of insulation [5]. Space charge and conduction current existence causes it's aging and reduces the time to breakdown [6]. Therefore, designed HVDC cable insulation should have no or negligible space charge accumulation and conduction current. Nanocomposites of epoxy, low-density polyethylene (LDPE) and so on have attracted the researcher's attention for the aforesaid application due to their favourable performance, such as increased dielectric strength, reduced dielectric loss, less space charge accumulation and so on [7–10]. In this study, un-modified XLPE/silica nanocomposites have shown increased breakdown strength, high partial discharge resistance and marginally suppressed space charge [11]. Space charge study hypothesises that nanofillers introduce deep traps, which inhibits the transport of charge carriers (electrons). Recent findings suggest that the surface modification of SiO_2 nanofillers (generally by silane) has further reduced the space charge [12–14]. Nonetheless, the choice of suitable nanofiller that will deliver optimal performance has still remained a challenge. In summary, there is an absence of detailed studies that explain the parameters taken into consideration for specific nanofiller selection. On the other side, conductivity (or conduction current) study of surface-modified XLPE nanocomposites is very limited [12] and is mostly reported for its un-modified nanocomposites [15–17]. The enhanced performance is attributed to high aspect ratio, large interaction zone and uniform dispersion due to surface modification (i.e. enhanced chemical bonding between polymer and nanofiller) of nanofillers. However, the parameters considered in certain nanofiller selection still remain indistinct. Identification of such parameter may stand as a tool to select suitable nanofiller for the intended application that can deliver the optimal performance of nanocomposites.

With this context, this paper proposes a nanofiller permittivity as a selection parameter that reduces space charge accumulation and conductivity suitable for HVDC cables. Space charge accumulation (measured by pulse-electro-acoustic (PEA) method) and conduction current (measured by the three-electrode setup) of surface-modified XLPE-silica and XLPE-MgO nanocomposites subjected to 20 kV/mm electric field is presented. Hereafter, octylsilane (OS) modified silica and (3-aminopropyl) triethoxy-silane modified (APTES) MgO nanocomposites are referred to as XLPE-OS-silica and XLPE-APTES-MgO nanocomposites, respectively.

2 Preparation and experimental details

2.1 Materials and preparations

LDPE granules obtained from Kalpena Industries Ltd., Calcutta have a density of 0.922 g/cm^3 and a melting point of 120°C. The literature reports that metal-oxide nanofillers such as silica, MgO marginally reduce the space charge accumulation in XLPE. Hence,

they are selected for this study [11–19]. As-received OS-modified silica nanofillers of diameter 7–14 nm and MgO nanofillers (un-modified) with the diameter of ∼30 nm were supplied by Reinste Nano Ventures Pvt. Ltd., New Delhi, India.

2.2 Surface modification of nanofillers

As the silica nanofillers as supplied by the supplier were surface modified by OS, its surface treatment is not carried and discussed here. However, as-received MgO nanofillers were not surface modified. Hence, its surface modification was done by the coupling agent APTES (code name – KH550). The procedure followed was as follows: initially, 10 g of MgO nanofillers was vacuum-dried at 373 K for 24 h before being dispersed in 100 ml toluene by sonication for 1 h. Then, KH550/toluene mixture (5 ml/50 ml) was added to nanofiller and then heated in an oil bath at 373 K and stirred for 24 h. Finally, nanofillers were collected by centrifugation, washed with toluene to remove excess coupling agent and dried under vacuum at 333 K for 24 h [20].

2.3 Nanocomposite preparation

XLPE nanocomposites were prepared by the melt blending method as follows: Both nanofillers were dried in the oven at 60°C for 24 h prior to its use. LDPE and nanofillers were mixed in two roll milling machine at 110°C for 10 min, and then crosslinking agent dicumyl peroxide (DCP) was added and mixed for 10 min. Hot pressing was used at 180°C with the pressure of 5–7 MPa for 30 min to allow uniform flow and full crosslinking. Samples of variable thickness ranging from 175 to 325 μm have been obtained. Different wt% compositions were obtained as follows: e.g. 1 wt% composition of XLPE-OS-silica nanocomposites contains 1 g of silica nanofillers and 99 g of LDPE granules with DCP.

2.4 Space charge and conduction current measurement

PEA (Flat specimen PEA system, TechImp Systems, Italy) method is used for space charge measurement [21]. The voltage signal received at the ground electrode is proportional to space charge density and is obtained using calibration and de-convolution through MATLAB code. The area of inner and outer electrodes is 750 and 850 cm^2, respectively. Thin aluminium foil of 50 μm is pasted on each sample, which acts as the electrode. Silicon oil drop is put on the electrodes to obtain a better acoustic signal. Space charge measurement is performed by applying 20 kV/mm for 1 h (polarisation time) and then switching off the supply and short-circuiting the sample for 1 h (depolarisation time). Polarisation and depolarisation currents are measured using Keithley 6517A electrometer by three-electrode setup [22] having outer and inner electrode diameters of 10 and 6.5 cm, following the same electric field (20 kV/mm), procedure and time (1 h for polarisation and depolarisation) as that of space charge measurement.

The values of an electrical field to be applied (20 kV/mm), polarisation and depolarisation time (1 h each) duration are selected considering the safety of the available DC source (max. 7 kV). In this study, 325 μm is the maximum thickness, which means 20 kV/mm can be safely applied, i.e. 6.5 kV can be supplied from a DC source ($E = V/d$, 'E' – electrical field, 'V' – applied voltage, 'd' – thickness of sample). Also, Auge *et al.* [23] suggest that threshold field for space charge measurement using PEA system for XLPE insulation is 15 kV/mm. Hence, any field above the threshold value is considered suitable for the space charge measurement. Both measurements are carried out at the room temperature.

2.5 Estimated parameters

The following parameters extracted from space charge and conduction current measurement are used to develop a mechanism that explains reduced space charge accumulation and conduction current.

2.5.1 Average space charge density: Average space charge density is calculated from the space charge profile obtained through calibration and deconvolution by (1) [19]

$$q(t) = \frac{1}{L}\int_0^L |q_p(x,t)|\,\mathrm{d}x \tag{1}$$

where 0, L are the electrode positions and $q_p(x, t)$ is the space charge profile.

2.5.2 Apparent charge mobility: Apparent charge mobility is calculated by MATLAB code from average space charge density during depolarisation time (i.e. depolarisation characteristics). $\mathrm{d}q(t)/\mathrm{d}t$ is calculated from the slope of the depolarisation characteristics. Since the mobility is an approximate estimation of space charge travelling speed, it is called as apparent charge mobility and can be calculated by (2) [1, 24] as follows:

$$\mu = \frac{\epsilon}{q(t)2}\frac{\mathrm{d}q}{\mathrm{d}t} \tag{2}$$

where μ is the apparent charge mobility, ϵ is the permittivity of a sample and $q(t)$ is average space charge density at time t.

2.5.3 Conduction current and conductivity: Conduction current is the difference between polarisation and depolarisation currents as mentioned earlier. Conductivity can be calculated using conduction current by (3) [25]

$$\sigma \simeq \frac{\epsilon_0}{C_0 V_0}(|i_p(t) - i_d(t)|) \tag{3}$$

where ϵ_0 is the permittivity of free space, C_0 is the geometric capacitance of the test object, V_0 is the applied voltage, $i_p(t)$ and $i_d(t)$ are polarisation and depolarisation currents at time t, respectively.

3 Results and analysis

3.1 Sample characterisation

Better dispersion of the nanofillers helps to attain the optimal performance of nanocomposites. Generally, the dispersion of nanofillers is observed by scanning electron microscope (SEM). SEM used was SUPRAA 55 ZEISS SEM attached to OXFORD PENTA FEM system designed for image acquisition and energy dispersive X-ray (EDX) analysis. Fig. 1 shows the SEM characterisation of randomly selected specimens from this study.

However, it must be noted that well-dispersed nanofillers (as expected from the surface modification of nanofiller) cannot be clearly observed in Fig. 1, as SEM micrographs in this study cannot reveal anything <100 nm. Still, it is worthwhile to mention here that SEM analysis using higher magnification may reveal the better dispersion of the surface-modified nanofillers. However, the equipment limitations and instability of samples at higher magnifications (which produce obscure SEM images) have restricted SEM characterisation to micrographic level in this study. Hence, it can be said that Fig. 1 only shows the presence of nanofillers inside the polymer matrix and not the better dispersion of Silica/MgO nanofillers. Also, it should be noted that Figs. 1*a* and *b* does not display the agglomeration of nanofillers. It is the surface morphology of polymer (may be due to cross-linking) that resembles agglomeration like structure, i.e. the agglomerates can be easily identified by the concentration of spherically shaped nanofillers at a particular location.

3.2 Space charge

Space charge profile obtained from calibration and de-convolution of PEA signal is generally used for result analysis. As explained earlier, homo- and hetero-charge have the same and opposite polarity to that of the adjacent electrode, respectively. In this study,

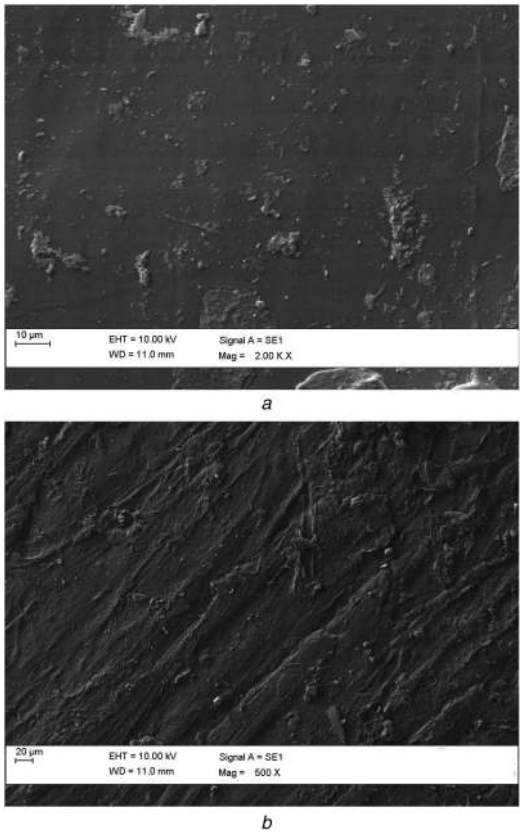

Fig. 1 *SEM characterisation of*
(a) XLPE-OS-silica 2 wt%, ***(b)*** XLPE-APTES-MgO 3 wt%

space charge measurement is done for 1 h each under the polarisation and depolarisation conditions. Hence, space charge profiles can be plotted from 0 to 60 min with the interval of 1 min. However, such representation of space charge profile may further complicate the result analysis, i.e. the increase or decrease of space charge signal amplitude (positive and negative) can be easily seen with the representation at the limited time instances. Therefore, only 0, 10, 30 and 60 min space charge profiles are shown in Figs. 2*a* and *b*. With this context, Fig. 2*a* shows that the pure XLPE has hetero-charge accumulation near the cathode. As discussed earlier, hetero-charge formation decreases the electrical field inside the insulation. Hence, the uneven distribution of electrical field leads to the premature aging of insulation that reduces its operating life. Such condition eventually poses threat to the entire power system in terms of quality of electrical power to be delivered and cost of replacement. Therefore, hetero-charge formation must be reduced or eliminated to maintain the uniformity of the electrical field inside the insulation. It is reported elsewhere that hetero-charge is formed due to acetophenone by-product formed during cross-linking. To explain, the decomposition of cross-linking agent DCP produces by-products such as acetophenone, α-methylstyrene and cumyl alcohol, which are responsible for space charge formation. Amongst them, acetophenone is responsible for hetero-charge accumulation [4]. It must be noted that samples are having a variable thickness ranging from 175 to 325 µm. However, it may not affect the space charge profile due to the lesser variation of thickness amongst the nanocomposites and less electrical field applied (20 kV/mm) in this study, i.e. different sample thicknesses can cause different breakdown strength of the samples. Findings of [26–28] suggest that µm range thickness may not affect the space charge profile and breakdown time of LDPE nanocomposites at room temperature. Similarly, XLPE nanocomposites under isothermal condition (both electrodes at the temperature of 20°C) exhibit very little variation in space charge profile (shown by the dotted red line) [29]. However, under the temperature gradient condition marginal variation is observed. However, this study is not carried under such

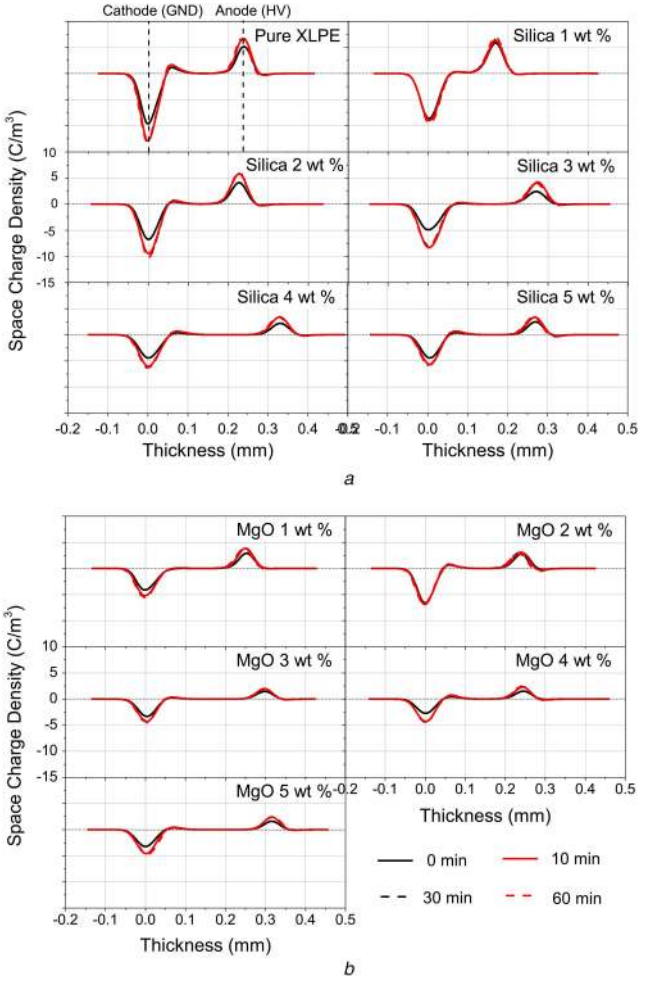

Fig. 2 *Space charge profile of*
(a) XLPE-OS-silica nanocomposites, ***(b)*** XLPE-APTES-MgO nanocomposites

condition. Hence, it can be said that the sample thickness may not marginally influence space charge accumulation.

Figs. 2*a* and *b* show the space charge profiles of XLPE-OS-silica and XLPE-APTES-MgO nanocomposites. It clearly shows that all nanocomposites have a lesser space charge accumulation (particularly hetero-charge) than pure XLPE. To elucidate, amplitude (or peak) of space charge signal of pure XLPE is approx. −12.5 C/m^3 at the cathode and 7.5 C/m^3 at the anode. For XLPE-OS-silica nano 5 wt% as shown in Fig. 2*a*, the amplitude varies from approx. −10 C/m^3 (maximum value at the cathode) to approx. 7 C/m^3 (maximum value at the anode). Similarly, the percentage reduction in space charge can be calculated. XLPE-OS-silica nanocomposites show maximum reduction at anode and cathode for nano 1, 2, 3, 4 and 5 wt% are as follows: anode (6.67, 20, 46.7, 50.6 and 6.67%), cathode (28, 18.4, 32, 48 and 20%), respectively. Similarly, for XLPE-APTES-MgO nanocomposites maximum reduction observed for nano 1, 2, 3, 4 and 5 wt% are as follows: anode (53.3, 57.3, 46.7, 33.3 and 30.6%), cathode (56, 40, 44, 62.4 and 61.6%). The aforementioned percentage is calculated using 60 min profile. In a summary, XLPE-APTES-MgO nanocomposites show better performance as compared to XLPE-OS-silica nanocomposites towards space charge suppression.

It is believed that the addition of nanofiller creates deeper traps, which restricts the movement of the space charge. To clarify, the shallow trap depth (i.e. lower binding energy) in case of pure XLPE facilitates the easy movement of space charge within the insulation. Hence, the average space charge inside pure XLPE is higher than its nanocomposites (explained later in this section). In case of nanocomposites, the nanofillers modify the trap distribution inside the polymer matrix and trap depth is lower (i.e. higher binding energy) than pure XLPE. Deep traps introduced by nanofillers restrict the movement of space charge due to their higher energy level. Also, the recombination of charge carriers is

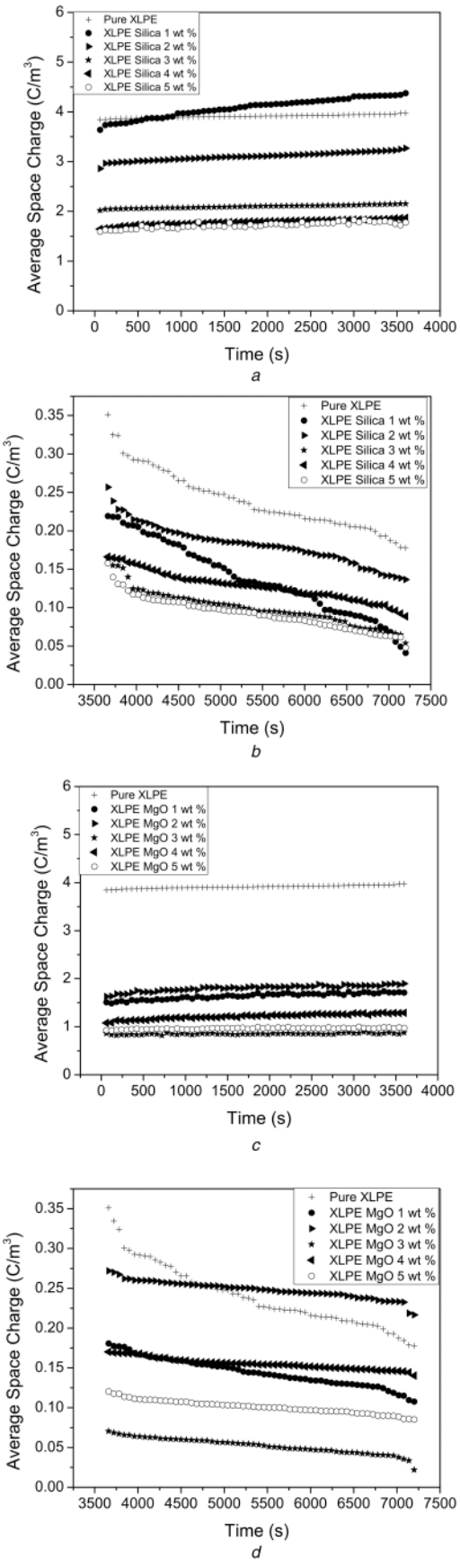

Fig. 3 *Average space charge density of* XLPE-OS-silica nanocomposites during ***(a)*** Polarisation, ***(b)*** Depolarisation and XLPE-APTES-MgO nanocomposites during ***(c)*** Polarisation, ***(d)*** Depolarisation

facilitated by nanofillers, i.e. the charge injection and extraction at respective electrodes is facilitated by nanofillers. This enhanced recombination of charge carriers helps to reduce space charge accumulation at anode and cathode. Space charge profile can also be expressed in terms of a quantity named as average space charge density. It is calculated using (1) that integrates the space charge over one complete space charge profile. Average space charge density calculated by (1) is plotted in Figs. 3*a–d*, respectively. As described earlier, polarisation and depolarisation are done for 1 h each hence, 60 data points can be observed in a complete polarisation and depolarisation period. It is recommended to study depolarisation curve to gain information about space charge since polarisation space charge density contains the capacitive charge of electrodes which may not reveal important phenomena such as recombination, trapping and so on [24].

Figs. 3*a–d* show that the average space charge density during polarisation and depolarisation remains well below pure XLPE. Average space charge density in the case of pure XLPE varies from 3.8 C/m^3 (minimum) to 3.9 C/m^3 (maximum) during polarisation. The least average space charge density in XLPE-OS-silica nanocomposites during polarisation can be seen in 5 wt%, which varies from 1.6 C/m^3 (minimum) to 1.7 C/m^3 (maximum) as shown in Fig. 3*a*. Similarly, Fig. 3*c* shows that 3 wt% has the least average space charge density (0.7 C/m^3 maximum to 0.8 C/m^3 minimum) amongst different XLPE-APTES-MgO nanocomposites during polarisation. Likewise, as shown in Figs. 3*b* and *d*, XLPE-APTES-MgO 3 wt% has the least average space charge density amongst all nanocomposites and pure XLPE during depolarisation. In summary, maximum reduction of ∼57.8% in average space charge density occurs inside 5 wt% of XLPE-OS-silica nanocomposites. Similarly, maximum 81.5% reduction of the same is observed in 3 wt% of XLPE-APTES-MgO nanocomposites as compared to pure XLPE. Clearly, XLPE-APTES-MgO nanocomposites show better performance than XLPE-OS-silica nanocomposites (clarification of this is explained in Section 5.2).

Hence from Figs. 3*a–d*, it can be inferred that the addition of nanofiller decreases space charge accumulation at respective electrodes. This is attributed to the restriction of charge carrier movement due to modified deeper traps created by the silica and MgO nanofillers. However, average space charge density in some of the nanocomposites is worthwhile to discuss here. For example, as shown in Fig. 3*b*, nano 1 wt% starts from low value and then reaches to the value even lower than nano 5 wt%, which is probably due to faster recombination of charge carriers.

It can be verified in Fig. 4*a*, i.e. the increased mobility of the charge carriers leads to its faster injection and extraction at respective electrodes. Apparent charge mobility represents the speed at which the charge carriers travel between the electrodes and the rate of injection and extraction at respective electrodes. Hence, Figs. 4*a* and *b* can be used to compare the apparent charge mobility of XLPE-OS-silica and XLPE-APTES-MgO nanocomposites. Figs. 4*a* and *b* clearly show that XLPE-OS-silica 5 wt% (in the range of 10^{-10}–10^{-11} m^2/V·s) and XLPE-APTES-MgO 3 wt% (in the range of 10^{-9}–10^{-10} m^2/V·s) show the highest apparent charge mobility that explains the least space charge accumulation inside them and average charge density amongst all nanocomposites.

Figs. 3*d* and *b* show that during depolarisation XLPE-APTES-MgO nanocomposites have less settling time (time to reach stable/constant value) with respect to the steady-state average space charge density as compared to XLPE-OS-silica nanocomposites, i.e. APTES-MgO nanofiller offer deeper traps than OS-silica nanofillers. This eases the recombination of charge carriers (i.e. electrons) and restricts its further movement.

In the case of XLPE-OS-silica and XLPE-APTES-MgO nanocomposites, nano 5 wt% and nano 3 wt% has the lowest space charge accumulation, respectively. It is reported elsewhere [11–14] that nanofiller inclusion leads to the introduction of deeper traps and high mobility of charges inside the sample. Due to increased mobility in case of XLPE-OS-silica and XLPE-APTES-MgO nanocomposites as shown in Figs. 4*a* and *b*, charges will travel at higher speeds and will get extracted at respective electrodes easily. Hence, there is very less or negligible homo- and hetero-space charge formation in the case of XLPE-APTES-MgO nanocomposites. To explain, charge injection and extraction at the respective electrodes is facilitated by the inclusion of nanofiller. It

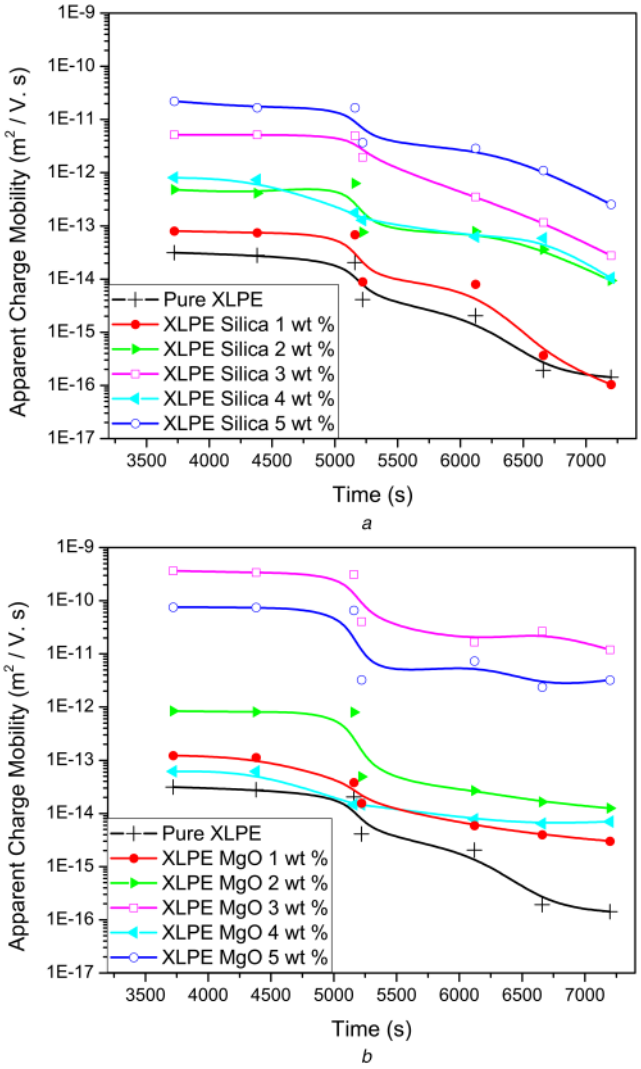

Fig. 4 *Apparent charge mobility of*
(a) XLPE-OS-silica nanocomposites, ***(b)*** XLPE-APTES-MgO nanocomposites

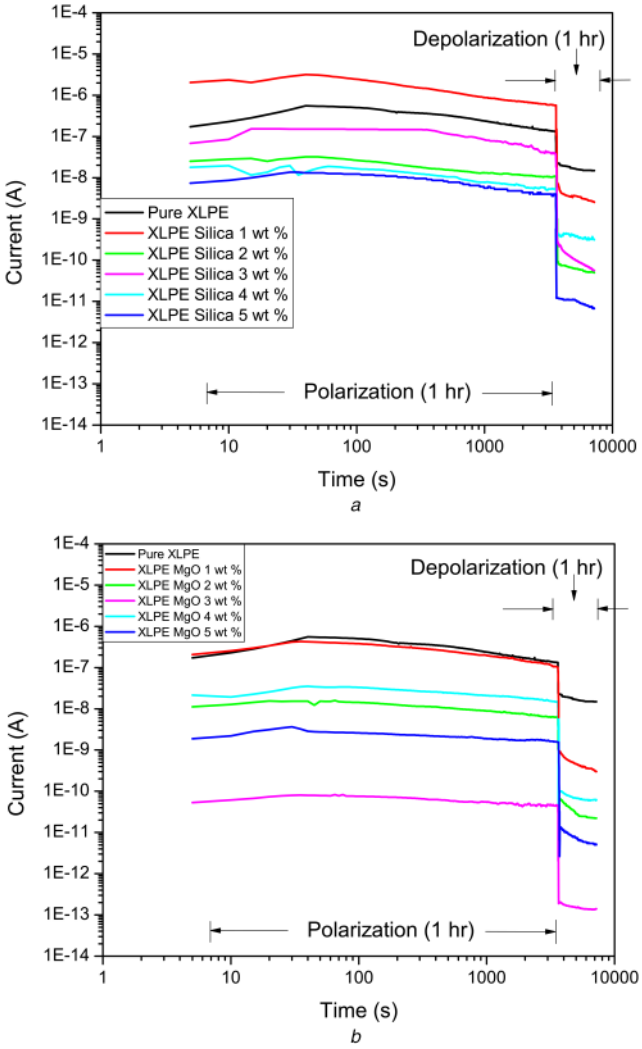

Fig. 5 *Polarisation–depolarisation current measurements of*
(a) XLPE-OS-silica nanocomposites, ***(b)*** XLPE-APTES-MgO nanocomposites

is clear that XLPE-OS-silica nano 5 wt% and XLPE-APTES-MgO nano 3 wt% have the highest mobility values and the lowest space charge accumulation. Better performance of XLPE-APTES-MgO nanocomposites over XLPE-OS-silica nanocomposites is explained later with the help of band gap theory.

4 Conductivity measurement

As explained, polarisation and depolarisation currents flow inside the insulation due to dielectric polarisation and relaxation phenomenon. Conduction current is the different between polarisation and depolarisation currents. Applying an electrical field and then removing the field measures the polarisation and depolarisation currents. High conduction current eventually poses danger to insulation and hence must be reduced. As discussed earlier in the case of polymers, the nanofiller addition decreases the conduction current. This is due to the introduction of nanofiller that induces deep traps than the polymer matrix, which captures the charge carriers. This mechanism ceases the flow of charges, which eventually decreases the flow of conduction current (explained in 'band gap theory model'). Equation (3) shows that the conductivity measurement is dependent on polarisation and depolarisation current values. Higher the conductivity more likely is the degradation probability of insulation. Hence, the conductivity (or conduction current) must be minimised in the case of insulation.

Figs. 5*a* and *b* show that the conduction current in all nanocomposites remains well below as compared to pure XLPE. Conduction current in pure XLPE remains in the range of 10^{-6}–10^{-7} A.

In the case of nanocomposites, it is least in 5 wt% (in the range of 10^{-8}–10^{-11} A) of XLPE-OS-silica nanocomposites, which is further reduced to the range of 10^{-10}–10^{-13} A in the case of 3 wt% of XLPE-APTES-MgO nanocomposites. Also, the same proportion can be observed in the case of the conductivity of nanocomposites.

As shown in Figs. 6*a* and *b*, the least conductivity is observed in 3 wt% (in the range of 10^{-15}–10^{-17} S/m) of XLPE-APTES-MgO nanocomposites and 5 wt% (in the range of 10^{-11}–10^{-12} S/m) of XLPE-OS-silica nanocomposites as compared to pure XLPE (in the range of 10^{-9}–10^{-10} S/m). It is believed that the nanofillers restrict the movement of charges that reduce the conduction current. Hence, it can be inferred from Figs. 5*a*, *b* and 6*a*, *b* that XLPE-OS-silica nano 5 wt% and XLPE-APTES-MgO nano 3 wt% have the least degradation probability due to lowest conductivity (or conduction current) values. In summary, the conductivity is decreased by approximately two orders in case of 5 wt% and by approximately six orders in case of 3 wt% of XLPE-APTES-MgO nanocomposites as compared to pure XLPE. The optimal performance of XLPE-APTES-MgO nanocomposites against XLPE-OS-silica nanocomposites is attributed to the less band gap of MgO nanofillers.

Nevertheless, the effect of transient behaviour of $i_p(t)$ and $i_d(t)$ on the conductivity measurement must be discussed here. Equation (3) shows that the conduction current is proportional to the conductivity. However, this may not be true in all cases of nanocomposites. For example, in the case of pure XLPE, $i_p(t)$ decreases rapidly and $i_d(t)$ decreases very slowly as compared to silica 3 wt%. Such behaviour is attributed to the charge carrier trapping and recombinations. To explain, the slowly decreasing

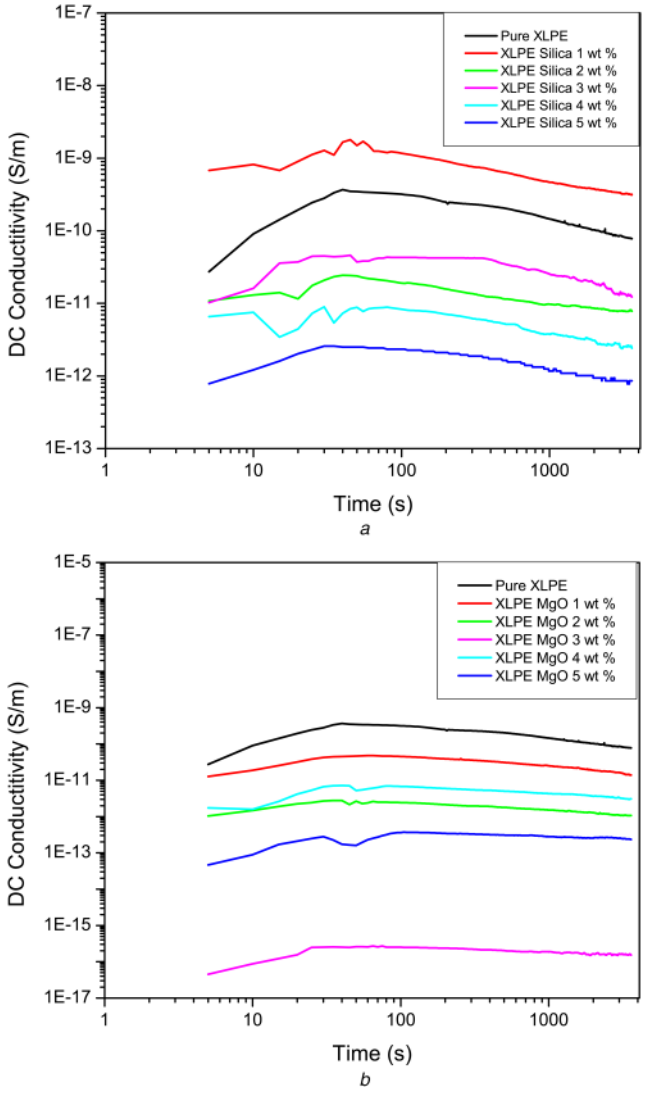

Fig. 6 *Conductivity of* ***(a)*** XLPE-OS-silica nanocomposites, ***(b)*** XLPE-APTES-MgO nanocomposites

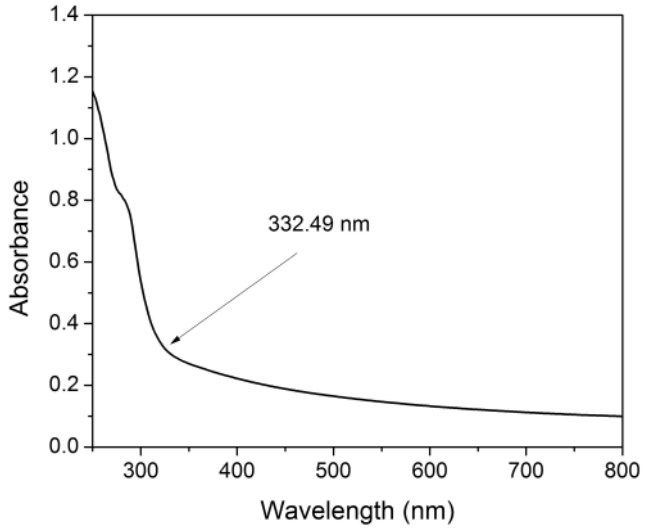

Fig. 7 *UV absorption spectra of XLPE-OS-silica nano 1 wt% nanocomposite*

behaviour of $i_d(t)$ in pure XLPE can be ascribed to the slow recombination of charge carriers. Similarly, rapidly decreasing $i_d(t)$ in silica 3 wt% can be attributed to the faster recombination of charge carriers. Sometimes, such behaviour may have repercussions on the conductivity results. Conductivity measurement results can be summarised as, in the case of XLPE-OS-silica nanocomposites 1 wt% > pure XLPE > 3 wt% > 2 wt% > 4 wt% > 5 wt% and pure XLPE > 1 wt% > 2 wt% > 4 wt% > 5 wt% > 3 wt% in the case of XLPE-APTES-MgO nanocomposites.

Table 1 Band gap values determined from UV spectroscopy

Nanofiller wt %	Band gap energy (eV) of XLPE-OS-silica nanocomposites	Band gap energy (eV) of XLPE-APTES-MgO nanocomposites
1	3.62	2.64
2	3.76	2.698
3	3.85	2.33
4	3.98	2.31
5	3.96	2.45

5 Band gap theory model

5.1 Band gap measurement

To develop a band gap theory model, the band gap must be calculated. It is calculated from absorption spectra of ultraviolet (UV) spectroscopy [29]. In this case, the energy equation of quantum mechanics is used, i.e.

$$E = \frac{hC}{\lambda} \tag{4}$$

where E is the band gap energy (eV); h is Planck's constant (6.626×10^{-34} J·s); C is the speed of light (3×10^8 m/s); and λ is the cut-off wavelength in UV absorption spectra (in nm).

Fig. 7 shows the UV spectra of XLPE-OS-silica nano 1 wt% from which band gap energy is calculated. Cut-off wavelength (λ) is the wavelength from which the complete cut-off of absorbance is observed [30], i.e. it is the threshold value from which absorbance starts to attain constant but minimum/zero value. Generally, it is the point on the curve (absorbance versus wavelength) at which the absorbance approaches zero. For example, as shown in Fig. 7, in the case of XLPE-OS-silica nano 1 wt%, a strong cut-off of absorbance is observed at 342.91 nm. It shows that from the wavelength of 342.91 nm the absorbance approaches to its zero value.

Similarly, cut-off wavelengths on the curve are measured for all samples which give the band gap values as shown in Table 1. It clearly shows that the XLPE-APTES-MgO nanocomposites have less band gap less than XLPE-OS-silica nanocomposites. The significance of the band gap in charge carrier recombination is discussed in the following section.

In a summary, XLPE-APTES-MgO nanocomposites are more favourable over XLPE-OS-silica nanocomposites for the HVDC cable insulation due to least space charge accumulation and conductivity (or conduction current). Albeit, no direct mathematical correlation between space charge accumulation and conduction current is developed hitherto, in [12] modifier TC9 and in [17] nano 1.5 phr (at room temperature) reports the lowest space charge accumulation and conductivity. Hence, it can be inferred that optimal performance towards space charge accumulation and conductivity can be obtained at same nanofiller wt%. However, this inference has to be verified by further studies.

From the economical point of view, it is important to know the selection parameter amongst different available nanofillers. Takada *et al.* in [18] have explained the effect of different parameters of nanofillers such as permittivity, diameter and shape on the trapping depth. It shows that nanofiller with the highest permittivity and diameter has maximum trapping depth. The same can be also applied to this study. With this context, the role of nanofiller permittivity in optimal performance of XLPE-APTES-MgO nanocomposites towards the space charge and conduction current measurement is explained with the help of band gap theory in the following section.

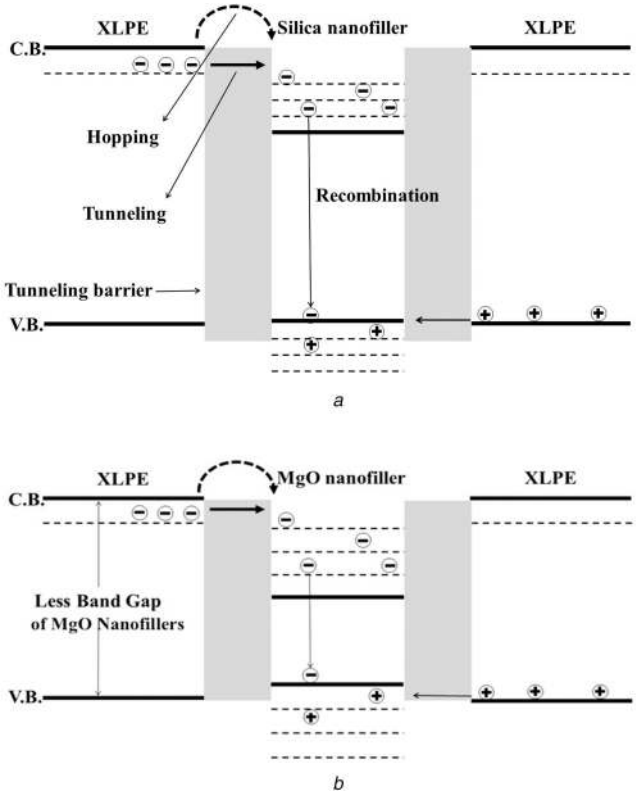

Fig. 8 *Band gap theory model for*
(a) XLPE-OS-silica nanocomposites, ***(b)*** XLPE-APTES-MgO nanocomposites

5.2 Discussion

Relative permittivity (ϵ_r) of OS modified silica and APTES modified MgO nanofiller is 4.1 and 10.3, respectively. ϵ_r of all samples is measured using LCR meter (Hioki, 3532-50) at 50 Hz (considering the value of vacuum permittivity as 8.854×10^{-12} F/m). Table 2 clearly shows that the XLPE-APTES-MgO nanocomposites have higher ϵ_r values as compared to XLPE-OS-silica nanocomposites. Results show that the XLPE-APTES-MgO nanocomposites show better performance as compared to XLPE-OS-silica nanocomposites, i.e. less space charge accumulation and low conductivity (or conduction current). This may be due to the higher ϵ_r value of MgO nanofillers. The role of nanofiller permittivity is discussed with the help of a band gap theory model.

Table 1 shows that the silica nanofiller has a higher band gap energy than MgO nanofiller. Figs. 8*a* and *b* show that the conduction through tunnelling phenomenon starts as localised energy states of nanofiller and XLPE electron become equal. As reported in [19, 31] nanofiller act as electron–hole recombination centres after the initiation of charge (i.e. electron) carrier conduction. Fig. 8*a* shows that due to the large band gap, recombination in XLPE-OS-silica nanocomposites will be a slow process and hence may take longer time for space charge to reach steady state. This assumption can be supported by Fig. 3*b*. Whereas in the case of XLPE-APTES-MgO nanocomposites, due to lesser band gap as shown in Fig. 8*b* the electron–hole recombination will be fast and space charge will reach steady state within less time as shown in Fig. 3*d*. Also, fast recombination in XLPE-APTES-MgO nanocomposites can be due to reduced tunnelling or potential barrier height. According to Arrhenius law as shown below:

$$\mu = \mu_0 e^{-\left(\frac{E_a}{kT}\right)} \tag{5}$$

where E_a is the potential barrier height; T is the temperature; k is Boltzmann constant and μ_0 is constant.

The role of nanofiller permittivity can also be verified by simulation study presented in [18]. It reports that higher nanofiller permittivity induces deeper trap depths (i.e. high energy level), particularly when the permittivity of nanofiller is more than two times of polymer. It can be interpreted from (5) that less potential barrier height (in eV) gives rise to increased mobility. Hence, in the case of XLPE-APTES-MgO nanocomposites, tunnelling barrier height is less as compared to XLPE-OS-silica nanocomposites. Less barrier height may allow easy passage of electrons through tunnelling or hopping. To correlate this conclusion with our present study, the space charge can get easily trapped inside MgO nanofiller due to higher permittivity (approximately three times of XLPE) than silica nanofiller. Also, Takada *et al.* [18] report that larger the diameter of the nanofillers, deeper will be the traps (i.e. with high energy level) created by it. In this study, MgO has a larger diameter (30 nm) than silica nanofiller (7–14 nm). This may also justify the better performance of XLPE-APTES-MgO nanocomposites against XLPE-OS-silica nanocomposites. However, a larger diameter may also mean less interfacial zone area available for interfacial reactions [7]. Hence, the diameter may not be a selection parameter of different available nanofillers for the present application. It should be noted that optimal performance in terms of space charge and conduction current may or may not always occur at the same wt% of nanofiller in respective nanocomposites (in this study XLPE-APTES-MgO nano 3 wt%) since it is dependent on the uniform dispersion of nanofiller inside the polymer matrix. To explain, no direct relation between space charge accumulation and conduction current is developed hitherto which would be of great interest in future studies. Hence, XLPE nanocomposites that include nanofillers such as $BaTiO_3$ ($\epsilon_r = 7000$) and TiO_2 ($\epsilon_r = 85.3$) can be experimented to know the effect of nanofiller permittivity on space charge and conductivity measurement due to their high nanofiller permittivity values.

Table 2 Relative permittivities of XLPE nanocomposites

Nanofiller wt %	Relative permittivity of XLPE-OS-silica nanocomposites	Relative permittivity of XLPE-APTES-MgO nanocomposites
pure XLPE	2.8	2.8
1	3.0	4.32
2	3.11	4.34
3	3.15	4.47
4	3.27	4.51
5	3.40	4.45

6 Conclusion

This paper presents an experimental study to show the effect of nanofiller permittivity on space charge and conduction current measurement of XLPE-OS-silica and XLPE-APTES-MgO nanocomposites. The following conclusions are drawn from this study:

i. MgO nanofiller has a higher permittivity than silica nanofiller. Hence, XLPE-APTES-MgO nanocomposites have less space charge accumulation and low conduction current than XLPE-OS-silica nanocomposites. Hence, former nanocomposites will have low degradation probability than later.
ii. In XLPE-OS-silica nanocomposites, nano 5 wt% has the lowest space charge accumulation and conductivity whereas XLPE-APTES-MgO has at nano 3 wt%. Hence, XLPE-APTES-MgO nanocomposites can also be considered as an economically viable solution.
iii. Maximum reduction by ∼57.8 and 81.5% in average space charge density occur inside 5 wt% of XLPE-OS-silica and 3 wt % of XLPE-APTES-MgO nanocomposites as compared to pure XLPE. Also, conductivity is decreased by approximately two and six orders in the case of aforesaid nanocomposites as compared to pure XLPE.
iv. Band gap theory model is presented to justify the role of nanofiller in the suppression of space charge accumulation and low conductivity. It shows that high permittivity of MgO nanofiller lowers the band gap and tunnelling barrier height,

which facilitates the recombination and trapping of charge carriers.

v. Hence, the nanofiller permittivity can be considered as a selection parameter to obtain optimal performance of XLPE nanocomposites for the intended application from the pool of different available nanofillers.

7 Acknowledgments

The authors thank Dr. C.C. Reddy from IIT Ropar for providing a facility for preparation of samples, Dr. Nandini Gupta from IIT Kanpur for availing the facility of space charge and conduction current measurement and Dr. S. Kalainathan from VIT University, Vellore for dielectric measurement.

8 References

[1] Montanari, G.C., Morshuis, P.H.F.: 'Space charge phenomenology in polymeric insulating materials', *IEEE Trans. Dielectr. Electr. Insul.*, 2007, **12**, (4), pp. 754–767

[2] Wang, X., Tu, D., Tanaka, Y., *et al.*: 'Space charge in XLPE power cable under DC electrical stress and heat treatment', *IEEE Trans. Dielectr. Electr. Insul.*, 1995, **2**, (3), pp. 467–474

[3] Montanari, G.C., Mazzanti, G., Palmieri, F., *et al.*: 'Space-charge trapping and conduction in LDPE, HDPE and XLPE', *J. Phys. D, Appl. Phys.*, 2001, **34**, (18), pp. 2902–2911

[4] Suh, K.S., Hwang, S.J., Noh, J.S., *et al.*: 'Effects of constituents of XLPE on the formation of space charge', *IEEE Trans. Dielectr. Electr. Insul.*, 1994, **1**, (6), pp. 1077–1083

[5] Montanari, G.C., Laurent, C., Teyssedre, G., *et al.*: 'From LDPE to XLPE: investigating the change of electrical properties. Part I. Space charge, conduction and lifetime', *IEEE Trans. Dielectr. Electr. Insul.*, 2005, **12**, (3), pp. 438–446

[6] Vu, T.T.N., Teyssedre, G., Le Roy, S., *et al.*: 'Space charge criteria in the assessment of insulation materials for HVDC', *IEEE Trans. Dielectr. Electr. Insul.*, 2017, **24**, (3), pp. 1405–1415

[7] Tanaka, T.: 'Dielectric nanocomposites with insulating properties', *IEEE Trans. Dielectr. Electr. Insul.*, 2005, **12**, (5), pp. 914–928

[8] Li, S., Zhu, Y., Min, D., *et al.*: 'Space charge modulated electrical breakdown', *Sci. Rep.*, 2016, **6**, pp. 1–4

[9] Li, H., Wang, C., Guo, Z., *et al.*: 'Effects of silane coupling agents on the electrical properties of silica/epoxy nanocomposites'. Proc. IEEE Int. Conf. Dielectrics (ICD), Montpellier, 2016, pp. 1036–1039

[10] Li, Z., Du, B., Han, C., *et al.*: 'Trap modulated charge carrier transport in polyethylene/graphene nanocomposites', *Sci. Rep.*, 2017, **7**, pp. 1–8

[11] Tanaka, T., Bulinski, A., Castellon, J., *et al.*: 'Dielectric properties of XLPE/SiO_2 nanocomposites based on CIGRE WG D1.24 cooperative test results', *IEEE Trans. Dielectr. Electr. Insul.*, 2011, **18**, (5), pp. 1482–1517

[12] Zhang, L., Zhou, Y., Huang, M., *et al.*: 'Effect of nanoparticle surface modification on charge transport characteristics in XLPE/SiO_2 nanocomposites', *IEEE Trans. Dielectr. Electr. Insul.*, 2014, **21**, (2), pp. 424–433

[13] Zhang, L., Zhou, Y., Cui, X., *et al.*: 'Effect of nanoparticle surface modification on breakdown and space charge behavior of XLPE/SiO_2 nanocomposites', *IEEE Trans. Dielectr. Electr. Insul.*, 2014, **21**, (4), pp. 1554–1564

[14] Zhang, L., Khani, M.M., Krentz, T.M., *et al.*: 'Suppression of space charge in crosslinked polyethylene filled with poly (stearyl methacrylate)-grafted SiO_2 nanoparticles', *Appl. Phys. Lett.*, 2017, **110**, (13), pp. 132903-1–132903-4

[15] Roy, M., Nelson, J.K., MacCrone, R.K., *et al.*: 'Candidate mechanisms controlling the electrical characteristics of silica/XLPE nanodielectrics', *J. Mater. Sci.*, 2007, **42**, (11), pp. 3789–3799

[16] Hui, L., Nelson, J.K., Schadler, L.S.: 'The influence of moisture on the electrical performance of XLPE/silica nanocomposites'. 10th IEEE Int. Conf. on Solid Dielectrics, Potsdam, Germany, July 2010, pp. 1–4

[17] Yan, Z., Han, B., Zhao, H., *et al.*: 'Space charge and conductivity characteristics of CB/XLPE nanocomposites'. Proc. Int. Symp. on Electrical Insulating Materials, Niigata, June 2014, pp. 30–33

[18] Takada, T., Hayase, Y., Tanaka, Y., *et al.*: 'Space charge trapping in electrical potential well caused by permanent and induced dipoles for ldpe/mgo nanocomposite', *IEEE Trans. Dielectr. Electr. Insul.*, 2008, **15**, (1), pp. 152–160

[19] Andritsch, T., Kochetov, R., Lennon, B., *et al.*: 'Space charge behavior of magnesium oxide filled epoxy nanocomposites at different temperatures and electric field strengths'. Electrical Insulation Conf., Annapolis, MD, August 2011, pp. 136–140

[20] Chen, S.S., Hu, J., Gao, L., *et al.*: 'Enhanced breakdown strength and energy density in PVDF nanocomposites with functionalized MgO nanoparticles', *RSC Adv.*, 2016, **6**, (40), pp. 33599–33605

[21] ASTM Standard D 257: 'Standard test methods for DC resistance or conductance of insulating materials', 1993

[22] Recommended Practice for Space Charge Measurements in HVDC Extruded Cables for Rated Voltages Up to 550 kV, IEEE Standard 1732, IEEE DEIS TC/WG 'HVDC Cable Systems', June 2017

[23] Auge, J.L., Laurent, C., Fabiani, D., *et al.*: 'Investigating dc polyethylene threshold by space charge. Current and electroluminescence measurements', *IEEE Trans. Dielectr. Electr. Insul.*, 2000, **7**, (6), pp. 797–803

[24] Mazzanti, G., Montanari, G.C., Alison, J.M.: 'A space- charge based method for the estimation of apparent mobility and trap depth as markers for insulation degradation-theoretical basis and experimental validation', *IEEE Trans. Dielectr. Electr. Insul.*, 2003, **10**, (2), pp. 187–197

[25] Saha, T.K., Purkait, P.: 'Investigation of polarization and depolarization current measurements for the assessment of oil-paper insulation of aged transformers', *IEEE Trans. Dielectr. Electr. Insul.*, 2004, **11**, (1), pp. 144–154

[26] Yoshida, J., Maezawa, T., Miyake, H., *et al.*: 'Space charge accumulation and breakdown in LDPE and LDPE/MgO nano-composite under high dc stress at various temperatures'. IEEE Conf. on Electrical Insulation and Dielectric Phenomena, CEIDP'09, Virginia Beach, VA, USA, 2009, pp. 150–153

[27] Kanegae, E., Ohki, Y., Tanaka, T., *et al.*: 'Space charge behavior in multi-layered dielectrics with LDPE and LDPE/MgO nanocomposites?'. 10th IEEE Int. Conf. on Solid Dielectrics (ICSD), Potsdam, Germany, 2010, pp. 1–4

[28] Ohki, Y., Ishimoto, K., Kanegae, E., *et al.*: 'Suppression of packet-like space charge formation in LDPE by the addition of magnesia nanofillers'. IEEE 9th Int. Conf. on the Properties and Applications of Dielectric Materials (ICPADM), Harbin, China, 2009, pp. 9–14

[29] Lv, Z., Wu, K., Wang, X., *et al.*: 'Thickness dependence of space charge in XLPE and its nanocomposites under temperature gradient'. IEEE Int. Conf. on Solid Dielectrics (ICSD), Bologna, Italy, 2013, pp. 250–253

[30] Dharma, J., Pisal, A., Shelton, C.T.: 'Simple method of measuring the band gap energy value of TiO_2 in the powder form using a UV/Vis/NIR spectrometer', Application Note Shelton, CT: PerkinElmer, 2009

[31] Lewis, T.J.: 'A model for nano-composite polymer dielectrics under electrical stress'. Int. Conf. Solid Dielectrics, Winchester, UK, August 2007, pp. 11–14